This is the accepted version of the following article: Murza A, Besserer-Offroy É, Côté J, Bérubé P, Longpré JM, Dumaine R, Lesur O, Auger-Messier M, Leduc R, Sarret P, and Marsault É. (2015), C-terminal Modifications of apelin-13 significantly change ligand binding, receptor signaling and hypotensive action. J Med Chem, 58(5):2431-40. doi: 10.1021/jm501916k, **which has been published in final form at** http://pubs.acs.org/doi/abs/10.1021/jm501916k

C-terminal modifications of apelin-13 significantly change ligand binding, receptor signaling and hypotensive action

Alexandre Murza,[§,¥] Élie Besserer-Offroy,[§,¥] Jérôme Côté,[§,¥] Patrick Bérubé,[§,¥] Jean-Michel Longpré,[§,¥] Robert Dumaine,[§] Olivier Lesur,[#] Mannix Auger-Messier,[#] Richard Leduc,[§,¥] Philippe Sarret[§,¥,*] and Éric Marsault[§,¥,*]

[§] Département de Pharmacologie et Physiologie, Faculté de médecine et des sciences de la santé, Université de Sherbrooke, QC, Canada

[#] Département de Médecine, Faculté de médecine et des sciences de la santé, Université de Sherbrooke, QC, Canada

[¥] Institut de Pharmacologie de Sherbrooke, 3001 12[e] av nord, Sherbrooke (QC), Canada J1H 5N4

* Contributed equally to this work.

Corresponding author:

Prof. Éric Marsault

Tel: +1 819.821.8000 ext 72433

Fax: +1 819.564.5400

Email: eric.marsault@usherbrooke.ca

KEYWORDS: apelin, APJ, signaling, hypotension, structure-activity relationships.

ABBREVIATIONS USED

GPCR: G protein-coupled receptor, cAMP: Cyclic adenosine monophosphate, CHO: Chinese hamster ovary, HEK: Human embryonic kidney, MAP: Mean arterial pressure, ACE2: Angiotensin-converting enzyme type 2, ERK1/2: Extracellular signal-regulated kinases 1/2, DIAD: diisopropylazodicarboxylate, DCM: dichloromethane, DIPEA: *N,N*-diisopropylethylamine, DMF: *N,N*-dimethylformamide, HATU: O-(7-azabenzotriazol-1-yl)-1,1,3,3-tetramethyluronium hexafluorophosphate, TFA: Trifluoroacetic acid, TIPS: Triisopropylsilane, TBME: *tert*-butyl methyl ether, HPLC: High performance liquid chromatography, HRMS: High resolution mass spectrometry, FRET: Fluorescence resonance energy transfer, BRET: Bioluminescence resonance energy transfer, ATP: Adenosine triphosphate, AUC: Area under the curve.

ABSTRACT

Apelin is the endogenous ligand of the APJ receptor, a member of the G protein-coupled receptor family. This system plays an important role in the regulation of blood pressure and cardiovascular functions. To better understand the role of its C-terminal Phe^{13} residue on ligand binding, receptor signaling and hypotension, we report a series of modified analogs in which Phe^{13} was substituted by unnatural amino acids. These modifications delivered new compounds exhibiting higher affinity and potency to inhibit cAMP accumulation compared to apelin-13. In particular, analogs Bpa^{13} or $(\alpha\text{-Me})Phe^{13}$ were 30-fold more potent to inhibit cAMP accumulation than apelin-13. $Tyr(OBn)^{13}$ substitution led to a 60-fold improvement in binding affinity and induced stronger and more sustained drop in blood pressure compared to apelin-13. Our study identified new potent analogs of apelin-13, which represent valuable probes to better understand its structure-function relationship.

INTRODUCTION

The apelin receptor (also known as the angiotensin receptor-like 1,hereafter called APJ) is a member of the rhodopsin-like G protein-coupled receptor (GPCR) superfamily.[1] Apelin-13 and -17 are the predominant forms of apelin in rat brain and in rat and human plasma.[2,3] The apelinergic system has been detected in numerous peripheral tissues such as the kidney, heart, pancreas, and lung. In the central nervous system, the apelin/APJ complex is mainly expressed in the hypothalamus and in the spinal cord.[4–8] In recent years, APJ has emerged as a potential therapeutic target to treat obesity and diabetes, as well as gastrointestinal diseases, cancer, and HIV infection.[9,10] However, its most notable implication is in cardiovascular diseases where it exerts hypotensive and positive inotropic effects.[11–14] Indeed, acute intravenous administration of apelin-13 to healthy volunteers and patients with heart failure causes coronary and peripheral vasodilation accompanied by a lowering of blood pressure.[15,16] These effects were preserved following activation of the renin/angiotensin system in patients with heart failure.[17] In rodents, intravenous injection of apelin-17 or -13 rapidly decreases the mean arterial pressure (MAP) via a nitric oxide (NO)-dependent mechanism.[18,7,19] This mechanism seems to play a protective role in hypertension since chronic pressure overload increased the expression of apelin in normal mice, yet induced progressive heart failure in addition to cardiac hypertrophy in apelin-deficient mice.[20] However, even if most studies in human reported decreased apelin levels in cardiovascular diseases, methodological differences and the short half-life of endogenous apelin *in vivo* make it difficult to draw definitive conclusions on the cellular and physiological mechanisms involved.[21] Nonetheless, these observations, summarized by a number of recent reviews,[10,21,22] strengthen the potential of the apelinergic system as a target for the treatment of cardiovascular diseases.

Owing to these important applications, a better knowledge of the structure-activity and structure-function relationships of apelin is essential to our understanding of the cellular and physiological processes associated with the activation of APJ. Of particular interest is the reported ability of a truncated analog of apelin-13 in which the C-terminal Phe^{13} residue has been deleted or substituted by an Ala residue, to suppress the decrease in MAP induced by apelin-13.[23] The same observation made on apelin-17 strengthens the role of the C-terminal amino acid in the modulation of MAP.[19] Apelin-13 is hydrolyzed in the presence of purified angiotensin-converting enzyme type 2 (ACE2), which cleaves the peptide between the Pro^{12} and the C-terminal Phe^{13} residues.[24] However, the physiological involvement of ACE2 in the *in vivo* metabolism of apelin-13 remains to be confirmed.

Binding of apelin to APJ triggers the inhibition of forskolin-induced cAMP production, defined as its canonical pathway,[6,25] and mediates intracellular signaling pathways through $G\alpha_{i/o}$- and $G\alpha_q$-mediated coupling, leading to the activation of downstream effectors such as ERK1/2, Akt, protein kinase C and phospholipase C.[6,26,27–29] Interestingly, different isoforms of apelin recruit both β-arrestin-1 and β-arrestin-2 but appear to induce APJ internalization through different intracellular trafficking routes.[30] Additionally to its impact on hypotensive action, the C-terminal Phe residue of apelin-13 was shown to play a central role on APJ internalization and β-arrestin recruitment.[31,32]

The structure of apelin was investigated by 2D NMR by Langelaan *et al*, who concluded that the Arg^2-Pro^3-Arg^4-Leu^5 fragment adopts a more ordered structure compared to other regions of the peptide.[33] The alanine scan performed on apelin-13 (Pyr^1-Arg^2-Pro^3-Arg^4-Leu^5-Ser^6-His^7-Lys^8-Gly^9-Pro^{10}-Met^{11}-Pro^{12}-Phe^{13}) pinpointed key residues involved in APJ receptor binding and inhibition of forskolin-induced cAMP accumulation. Replacement of Arg^2, Arg^4, and Leu^5 residues by alanine leads to a robust decrease in binding, cAMP production, and intracellular Ca^{2+} release, consistent with a role as pharmacophores.[6,34] Using molecular

modeling and site-directed mutagenesis, the importance of the two Arg residues of apelin-13 for interaction with APJ was underlined.[35] These conclusions were exploited to design macrocyclic APJ agonists and antagonists.[36–38] A structure-activity relationship study of the first semi-peptidic APJ agonist E339-3D6[39] led to the discovery of more potent and stable agonists for the cAMP pathway and APJ internalization.[40] While deciphering the degradation pattern of apelin-13 *in vitro* and *in vivo*, our group recently identified that the substitution of Phe[13] by unnatural amino acids significantly improved plasma stability.[41]

As detailed above and based on recent literature, the C-terminal Phe[13] residue is critical to fine-tune receptor function.[42–44] In order to better understand the role of this residue and how it modulates binding and signaling profiles as well as *in vivo* effects, we substituted Phe[13] with unnatural amino acids and studied the impact of these substitutions on binding and various signaling pathways as well as its impact on blood pressure.

RESULTS AND DISCUSSION

Synthesis

NB: to ease reading, stereochemistry of amino acids is L unless otherwise noted. Analogs were synthesized by the solid-phase strategy using Fmoc protected amino acids, as previously reported.[44] Briefly, starting from Tentagel S PHB resin, a Mitsunobu reaction in the presence of triphenylphosphine (PPh_3) and diisopropylazodicarboxylate (DIAD) allowed the attachment of the first Fmoc N-protected C-terminal residue. After capping unreacted hydroxyl groups with a mixture of DCM/Ac_2O/DIPEA, the Fmoc group was deprotected with 20% piperidine in *N,N*-dimethylformamide (DMF). The following Fmoc N-protected amino acids were then attached stepwise in the presence of [O-(7-azabenzotriazol-1-yl)-1,1,3,3-tetramethyluronium hexafluorophosphate] (HATU), *N,N*-diisopropylethylamine (DIPEA) in DMF. Final resin cleavage with simultaneous side-chain deprotections was performed with a mixture of TFA (trifluoroacetic acid)/H_2O/TIPS (triisopropylsilane). After precipitation in *tert*-butyl methyl ether (TBME), the crude product was purified by reverse-phase chromatography, leading to the desired compounds exhibiting purity > 95%, as determined by High Performance Liquid Chromatography (HPLC) and characterized by High Resolution Mass Spectroscopy (HRMS) (**Table 1**).

Effects of Phe^{13} modifications on binding affinity

In an effort to better understand the structure-activity relationship of the apelin-13 C-terminus on APJ signaling and to discover new pharmacological tools, the Phe^{13} moiety was substituted with several natural and unnatural amino acids in continuation of our previous works (**Figure 1**).[44] To prevent oxidation side-products generally associated with the presence of Met in peptides,[45] the Met^{11} residue was replaced by Nle (**Tables 1** and **2**). This modification (analog **1**) led to minor differences in affinity, cAMP inhibition and $G\alpha_{i1}$ activation (Table 2). First,

replacement of residue Phe[13] with lipophilic residues Ile, Leu, and Val (**2**, IC_{50} 11.4 nM; **3**, IC_{50} 7.9 nM; **4**, IC_{50} 18.2 nM) provided around 10-fold loss on binding affinity compared to apelin-13 (**Ape13**, IC_{50} 1.2 nM). This may suggest that these aliphatic side chains in C-terminus are either too short to fully occupy the binding pocket of APJ, or that a π-stacking interaction is replaced by a less favorable hydrophobic interaction. Introduction of electron-donating substituents (resonance or induction) on the aromatic ring with Tyr(OMe) and Phe(4-Me) residues (**5**, IC_{50} 0.60 nM; **6**, IC_{50} 0.25 nM) led to a minor improvement in binding affinity, contrasting with the hypothesis of an electron-rich binding pocket for APJ[31] and our previous observations[44] showing an improved binding affinity for electron-poor aromatic residues in place of Phe[13]. (Pyridyl)Ala replacements (**7**, IC_{50} 1.3 nM; **8**, IC_{50} 1.6 nM; **9**, IC_{50} 6.1 nM) provided affinities close to the parent peptide. To further probe the existence of putative π-π interactions between the C-terminal amino acid of apelin-13 and the binding pocket of APJ, the electron density of the aryl group of Phe[13] and its distance from the backbone of the peptide were varied. Thus, phenylglycine (Phg) analog **10** elicited a 10-fold loss on binding affinity **(**IC_{50} 14.3 nM), underlining that C-terminal side chain distance from the backbone of apelin-13 may be critical for interaction with APJ. On the other hand, increasing the electron density and steric hindrance of the C-terminal residue (**11** - **19**) led to the identification of very potent analogs. Indeed, Tyr(OBn) modification **12** induced a 60-fold improvement in binding affinity versus the native peptide (IC_{50} 0.02 vs 1.2 nM), making it the most potent APJ ligand reported to date. On the other hand, introduction of dihydroAnthranylAla moiety **15**, which possesses a higher volume and π-stacking abilities, elicited a >10-fold loss compared to apelin-13 (IC_{50} 13.7 nM), suggesting that there is a limit in terms of steric hindrance in the interaction with APJ. We were further interested in assessing the impact of disubstitution at the α-carbon. To this end, residue Phe[13] was replaced by (α-Me)Phe, (D-α-Me)Phe, and aminoindane (**17**, IC_{50} 0.43 nM; **18**, IC_{50} 0.86 nM; **19**, IC_{50}

1.7 nM, respectively). These analogs exhibited IC_{50} close to that of apelin-13, suggesting that substitution of the Cα atom has a neutral effect on interactions with APJ.

Effects of apelin-13 Phe^{13} modifications on cAMP inhibition and Gα$_{i1}$ activation

The new analogs were then tested for their ability to inhibit forskolin-induced cAMP accumulation and to activate $G\alpha_{i1}$ dissociation using Fluorescence and Bioluminescence Resonance Energy Transfer assays (FRET and BRET, respectively)[32] (**Table 2, Figure 2**). Essentially, the effect of modifications at position 13 on these two pathways paralleled the trends observed in binding affinities. However, several analogs diverged from this trend, revealing that the C-terminal position of apelin-13 could also be involved in fine-tuning of the cAMP canonical pathway. Indeed, replacement of Phe^{13} with Phg (**10**) led to a 10-fold loss in binding while preserving cAMP potency (EC_{50} 2.7 nM) close to that of the parent peptide (**Ape13**, EC_{50} 1.4 nM). Likewise, substitution by homo-phenylalanine (hPhe, **11**) provoked an interesting improvement in cAMP potency (EC_{50} 0.24 nM) compared to apelin-13, despite a decreased affinity (IC_{50} 6.7 nM). Substitution of residue Phe^{13} by Bpa (**13**) or (α-Me)Phe (**17**) led to the two most potent analogs of apelin-13 described to date, exhibiting around 30-fold improvement on inhibition of cAMP production (**13**, EC_{50} 0.04 nM; **17**, EC_{50} 0.07 nM) compared to the native peptide. In contrast, the ability of dihydroAnthranylAla^{13} (**15**) to inhibit cAMP accumulation (EC_{50} 95 nM) was reduced by almost two orders of magnitude compared to apelin-13 despite a high binding affinity, which makes it an interesting pharmacological probe. An explanation could be related to the Black & Leff model[46] describing the relationship between biological responses and occupancy rate of a receptor (aka the "occupancy theory"), which states that some analogs could elicit a percentage of biological response higher than the percentage of receptor occupancy.[47] Additionally, during binding experiments, analogs compete with a radioligand possessing two modifications versus the natural ligand (Met^{11}Nle, Phe^{13}Tyr), whereas in the cAMP assays they are directly acting

on APJ. This could contribute to some of the differences observed between binding affinity and cAMP inhibition values.

The dissociation of $G\alpha_{i1}$ from $G\beta\gamma$ subunits induced by C-terminally modified analogs was also assessed using a BRET-based biosensor.[48] Typically, Phe^{13} replacements led to low nM potency on the $G\alpha_{i1}$ pathway close to apelin-13 (**Ape13**, EC_{50} 0.84 nM), suggesting that the C-terminal moiety of apelin-13 is not critical for $G\alpha_{i1}$ dissociation from the $G\beta\gamma$ subunits (**Table 2**, **Figure 2**). $G\alpha_{i1}$ engagement would be expected to correlate with the downstream inhibition of cAMP production. Nevertheless, several analogs showed remarkable disparities, suggesting that inhibition of cAMP production may also occur through another G-protein subtype or even through a G-protein-independent mechanism. The (α-Me)Phe analog (**17**) is 40-fold less potent to activate $G\alpha_{i1}$ than to decrease cAMP production ($G\alpha_{i1}$ EC_{50} 2.7 nM vs. cAMP EC_{50} 0.07 nM). This observation held true, to a lesser extent, when residue Phe^{13} was substituted by Bpa (**13**, $G\alpha_{i1}$ EC_{50} 0.91 nM vs. cAMP EC_{50} 0.04 nM). The structural differences between Bpa and (α-Me)Phe side-chains are obvious. However, both compounds were effective in activating a cAMP-dependent pathway, possibly via an alternative mechanism involving the recruitment of other G protein subunits. Indeed, adenylate cyclase (AC), which possesses nine isoforms in human,[49] is responsible for the conversion of ATP into cAMP and can be inhibited through various G protein-dependent mechanisms.[50] Other α subunits such as $G\alpha_{i2,3}$ or $G\alpha_o$ as well as the $G\beta\gamma$ subunits were demonstrated, in some cases, to have the ability to reduce intracellular levels of cAMP.[51,52] In contrast, dihydroAnthranyl^{13} (**15**), which exhibited an important loss in cAMP production inhibition, engaged $G\alpha_{i1}$ similarlyto apelin-13 ($G\alpha_{i1}$ EC_{50} 6.0 nM vs. cAMP EC_{50} 95 nM). This observation also leads to the hypothesis that $G\alpha_{i2,3}$ and/or $G\alpha_o$ would trigger the inhibition of cAMP production by apelin analogs in HEK293 cells.

N-terminal truncated analogs of Tyr(OBn) (12) exhibit drastic decrease in receptor binding

Substitution of residue Phe^{13} of apelin-13 by Tyr(OBn) (**12**) significantly improved its binding affinity to APJ (IC_{50} 20 pM). It is now accepted that the N-terminal fragment Arg^2-Pro^3-Arg^4-Leu^5 is an important pharmacophore.[6,33] The next question was whether the improved potency due to Tyr(OBn) could outweigh the contribution of N-terminal pharmacophoric elements. Thus, analog **12** was sequentially truncated starting from its N-terminal (**Table 3**). Deletions of the Pyr^1-Arg^2-Pro^3 amino acids dramatically decreased affinity for APJ (**20**, IC_{50} 57 nM vs. **12**, IC_{50} 0.02 nM). This 2800-fold loss was unexpected since Medhurst and coworkers described that the mutation Arg^{2}Ala in apelin-13 only led to a 50-fold decrease compared to the parent peptide.[6] The Pyr^{1}residue appears to play no crucial role in the interaction with APJ. However, it was described that deletion of Pyr^1-Arg^2 residues in apelin-13 led to an important decrease in affinity, suggesting that the absence of Arg^2 could be responsible for this considerable loss.[19,35] Furthermore, the Pro^3 residue appears to play a critical structuring role, as revealed by NMR studies which suggests a high level of rigidity within the Arg^2→Leu^5 fragment.[33] Thus, our results support the conclusions drawn from previous works. Moreover, deletion of Arg^4-Leu^5 amino acids completely abrogated binding (**21**, IC_{50} >10 µM). As expected, more heavily truncated analogs, **22** and **23**, also exhibited affinities >10 µM.

Signaling signature and hypotensive effects of apelin-13 and Tyr(OBn) analog (12)

We investigated further the signaling pathways triggered by the high-affinity analog Tyr(OBn) (**12**) using BRET biosensors. Indeed, we evaluated the engagement of $G\alpha_{i1}$ and $G\alpha_{oA}$ subunits as well as the recruitment of proteins involved in GPCR internalization, β-arrestin-1 and β-arrestin-2 (**Figure 2**). Whereas compound **12** induced an activation of the $G\alpha_{i1}$ subunit and a recruitment of β-arrestin-2 close to that elicited by apelin-13 (**Figure 2C**, **2F**), the inhibition of cAMP accumulation, the engagement of $G\alpha_{oA}$ subunit and the recruitment of β-arrestin-1induced by (**12**) appeared to be more potent as represented by the

concentration-response curves (**Figures 2B**, **2D**, **2E**). **Figure 2A** recapitulates potencies (EC_{50}) on the five signaling pathways tested. Interestingly, analog **12** which induced a 60-fold improvement in binding affinity versus apelin-13, did not possess increased potency on those signaling pathways in the same proportions.

The C-terminal amino acid was demonstrated to be capital for the hypotensive effect of apelin in spontaneously hypertensive rats, since its substitution by alanine or its deletion abrogated the reduction in mean arterial pressure (MAP).[23] The aromatic side chain of Phe^{13} seems to play a central role in this phenomenon. In order to assess the influence of the Tyr(OBn) replacement on MAP, apelin-13 and analog **12** were intravenously administered at doses of 0.001, 0.01, 0.1 and 1 mg/kg into Sprague-Dawley rats, then the systolic, diastolic, and mean arterial pressure were measured every 30 seconds with a tail-cuff non-invasive blood pressure system (**Figure 3**).[53] Dose-response curves revealed that injection of apelin-13 lowered MAP in a dose-dependent manner and that the maximal hypotensive effect was reached rapidly 1 minute after administration (**Figure 3A**). Apelin-13 induced 40, 30, and 20 mmHg decrease in MAP at doses of 1, 0.1, and 0.01 mg/kg, respectively.[54] At equal dose, analog **12** caused a marked reduction in MAP compared to apelin-13 (**Figure 3B**). Statistical analysis demonstrated that the MAP decrease was both stronger and more sustained for the Tyr(OBn) analog compared to apelin-13, as demonstrated by the determination of the area under the curve (AUC) for analog **12** at doses of 0.1 and 1 mg/kg (**Figure 3C**). The more sustained effect may be attributed to improved stability of **12** compared to **Ape13**. Indeed, we previously demonstrated that C-terminally modified analogs of apelin-13 possessed drastically increased plasma stabilities.[41] Particularly, the half-life of Tyr(OBn) analog **12** was superior to 1h ($t_{1/2}$ 66 min) whereas that of apelin-13 was close to 14 min in rat plasma.

Finally, the significantly higher potency of β-arrestin-1 recruitment elicited by analog **12** (β-arr1 EC_{50} 7.4 nM) compared to apelin-13 (β-arr1 EC_{50} 26 nM) correlates with its higher

hypotensive actions (**Figure 2A**). These observations are supported by previous work showing that the drop in MAP caused by C-terminally modified apelin peptides depends on the ability of those ligands to induce APJ internalization.[19,23] To reinforce this hypothesis, Ceraudo and co-workers recently suggested that the signaling pathways involved in apelin-17-induced MAP could be β-arrestin-dependent.[32] Altogether, our results reveal that analog **12** represents a more stable pharmacological tool to better understand the link between chemical structure, receptor signaling, and physiological function.

CONCLUSION

In this study, we report C-terminally modified analogs of apelin-13, with a particular focus on diverse unnatural aromatic amino acids as probes to further investigate the impact on binding, inhibition of forskolin-induced cAMP accumulation, activation of $G\alpha_{i1}$ subunit and *in vivo* activity. This led to the discovery of new apelin-13 analogs possessing pM-level binding and inhibition of cAMP production. Substitution of residue Phe^{13} by Bpa or (α-Me)Phe provided potent compounds exhibiting 30-fold improvement in inhibiting cAMP production and having high affinities for APJ. Furthermore, substitution of Phe^{13} by $Tyr(OBn)^{13}$ led the strongest binding affinity for APJ reported to date (IC_{50} 20 pM), 60-fold higher than the parent peptide. The latter was subsequently assessed for its ability to engage $G\alpha_{oA}$ subunit and to recruit β-arrestin-1 and β-arrestin-2. While its potency to recruit β-arrestin-2 and to activate $G\alpha_{i1}$ proteins was close to that of apelin-13, the Tyr(OBn) modification improved significantly the efficacy to inhibit cAMP production, to engage $G\alpha_{oA}$ subunit and to recruit β-arrestin-1. Finally, apelin-13 and its $Tyr(OBn)^{13}$ analog were administered to anesthetized rats to assess the impact on blood pressure. $Tyr(OBn)^{13}$ analog **12** lowered mean arterial blood pressure more robustly than apelin-13. Moreover, the hypotensive action of **12** was more sustained in time, an observation tentatively attributed to improved plasma stability compared to apelin-13. This study further supports previous works suggesting that the C-terminal amino acid is crucial for the hypotensive action of apelin. Overall, the analogs reported in this study constitute very interesting pharmacological tools to better understand the signaling pathways involved in the hypotensive effects and the physiological roles of the apelinergic system, as well as its ultimate validation as a pharmacological target for the treatment of cardiovascular diseases.

EXPERIMENTAL SECTION

Procedures for solid phase synthesis

Materials

Protected amino acids and TentaGel S PHB, O-[4-(Hydroxymethyl)phenyl]polyethylene glycol polystyrene resin were purchased from ChemImpex International (USA). All other reagents were purchased from Sigma-Aldrich (Canada), Fisher Scientific (USA) or ACP (Canada), were of the highest commercially available purity and were used as such. Peptide synthesis was performed in 12 mL polypropylene cartridge with 20 µm PE frit from Applied Separations (USA).

Peptide synthesis

TentaGel S PHB, O-[4-(Hydroxymethyl)phenyl]polyethylene glycol resin (0.27 mmol/g, 0.2 g) was treated with triphenylphosphine (5 equiv.), diisopropylazodicarboxylate (DIAD, 5 equiv.), Fmoc-protected amino acid (5 equiv.) in tetrahydrofuran (THF, 4 mL). The mixture was shaken overnight on an orbital shaker at room temperature, then the resin was sequentially washed for 3-min periods with DCM (2x 5 mL), toluene (1x 5 mL), EtOH (1x 5 mL), toluene (1x 5 mL), DCM/MeOH (75/25, 1x 5 mL), THF/MeOH (75/25, 1x 5 mL), DCM/MeOH (75/25, 1x 5 mL), THF/MeOH (75/25, 1x 5 mL), DCM (2x 5 mL). The resin was then capped with DCM/Ac_2O/DIPEA (20/5/1, 5 mL) at room temperature during 1 h, and washed with DCM (3x 5 mL), DCM/MeOH (75/25, 5 mL), DCM (3x 5 mL). After Fmoc deprotection with 20% piperidine/DMF (*N,N*-dimethylformamide) during 15 min, the following Fmoc-protected amino acid (5 equiv.) was attached in the presence of [O-(7-azabenzotriazol-1-yl)-1,1,3,3-tetramethyluronium hexafluorophosphate] HATU (5 equiv.), *N,N*-diisopropylethylamine (10 equiv.) in DMF (4 mL). Coupling reaction was run for 30 min

at room temperature, then piperidine (20% in DMF) was used to deprotect the Fmoc group at every step. The resin was washed after each coupling step and deprotection with DCM (2x 5 mL), 2-propanol (1x 5 mL), DCM (1x 5 mL), 2-propanol (1x 5 mL), DCM (2x 5 mL). For resin cleavage, the resin was treated with a mixture of TFA (trifluoroacetic acid)/H_2O/TIPS (triisopropylsilane), 95/2.5/2.5, v/v] (4 mL / 0.2 g of resin) for 4 h at room temperature. After filtration, peptide was precipitated in TBME (*tert*-butyl methyl ether) at 0°C, the suspension was centrifuged, the supernatant was removed and the crude product was re-dissolved in water. Purification by reverse-phase HPLC yielded the desire products as white powders after lyophilization.

Peptide purification and characterization

Crude peptides were purified by reverse-phase chromatography using a preparative HPLC from Waters (Autosampler 2707, Quaternary gradient module 2535, UV detector 2489, fraction collector WFCIII) equipped with an ACE5 C_{18} column (250 x 21.2 mm, 5 µm spherical particle size) and water + 0.1% TFA and acetonitrile as eluents. Analytical HPLC chromatograms were recorded on an Agilent 1100 series equipped with UV detector set at 223 nm and an Agilent Eclipse Plus C_{18} column (3.0 x 50 mm, 2.7 µm spherical particle size column) using the following method (0→10 min: 2→50% acetonitrile; 10→14 min: 50→100%; 14→18 min: 100%; 18→19 min: 100→2%; 19→24 min: 2%). All analogs possessed UV purity >95% at 223 nm. Molecular weights of analogs were determined by mass spectrometry (Electrospray infusion ESI-Q-Tof from Maxis).

Binding and cAMP accumulation

Materials

High glucose Dulbecco's Modified Eagle Medium (DMEM), G418 and penicillin/

streptomycin were purchased from Invitrogen Life Technologies (Canada). Fetal bovine serum (FBS) and Hank's balanced saline solution (HBSS) were purchased from Wisent (Canada) and bovine serum albumin (BSA) was purchased from BioShop (Canada). 3-isobutyl-1-methylxanthine (IBMX), and forskolin were purchased from Sigma-Aldrich (Canada). Apelin-13[Glp^{65}, Nle^{75}, Tyr^{77}][^{125}I], white opaque 96-well half area plates, OptiPlate™-384 white opaque microplates and LANCE®*Ultra* cAMP kit were purchased from PerkinElmer (Canada). Polyethylenimine (branched PEI) was obtained from Polysciences (USA). Coelenterazine-400A (DeepBlueC) was purchased from Biosynth International Inc. (USA). BRET^2 measurements were performed on an M1000 plate reader from Tecan (USA).

Cell culture

Stably transfected HEK293 cells expressing the YFP epitope-tagged human APJ were cultured in high glucose DMEM supplemented with 10% FBS. Cells were kept in a humidified atmosphere with 5% CO_2 at 37^{o}C according to the manufacturer's instructions. G418 and penicillin/streptomycin were used as selection agent and antibiotics, respectively.

Radioligand binding

HEK293 cells expressing the YFP epitope-tagged human APJ were washed once with PBS and subjected to one freeze-thaw cycle. Broken cells were then gently scraped in resuspension buffer (1mM EDTA and 10 mM Tris-HCl, pH 7.5), centrifuged at 3500 g for 15 min at 4°C and resuspended in binding buffer (50 mM Tris-HCl buffer, pH 7.5, containing 0.2% BSA). Competition radioligand binding experiments were performed by incubating cell membranes (15 µg) with 0.2 nM Apelin-13[Glp^{65}, Nle^{75}, Tyr^{77}][^{125}I] (2200 ci/mmol) and increasing concentrations of various apelin analogs (10^{-12} to 10^{-6} M) for 1 h at room temperature in a

final volume of 200 µL. Bound radioactivity was separated from free ligand by filtration through glass fiber filter plates (Millipore, Billerica, MA) pre-soaked for 1 h in PEI 0.2% at 4°C and washed 3 times with 170 µL of ice-cold washing buffer (50 mM Tris-HCl buffer, pH 7.5, 0.2% BSA). Receptor-bound radioactivity was counted in a γ-counter 1470 Wizard form PerkinElmer (80% counting efficiency). Nonspecific binding was measured in the presence of 10^{-5} M unlabeled apelin-13 and represented less than 5% of total binding. IC_{50} values were determined from inhibition curves as the unlabeled ligand concentration inhibiting 50% of [^{125}I]-apelin-13 specific binding. All binding data were calculated and plotted using GraphPad Prism 6 and represent the mean ± SEM of three determinations. Inhibitions constants (K_i) of analogs were calculated using the Cheng-Prusoff equation.[55]

Measurement of cAMP production

Intracellular cAMP production was determined using PerkinElmer's LANCE®*Ultra* cAMP kit and following manufacturer's recommendations. Assays were performed in OptiPlate™-384 white opaque microplates. The stimulation buffer used for assays contained 1X HBSS, 0.5 mM IBMX and 0.1% BSA (pH 7.4). Cells (4 µL), at concentrations of 750 cells/well in stimulation buffer, were plated followed by forskolin (2 µL) at 1 µM in stimulation buffer. Increasing concentrations (10^{-12} to 10^{-6} M) of ligands (2 µL) were then added and the microplate was incubated at 37°C for 30 min. After stimulation, cells were lysed by successive additions of the Eu-cAMP tracer (4 µL) and the U*Light*-cAMP mAb (4 µL) prepared in the cAMP Detection Buffer provided with the kit followed by a 1h incubation at room temperature with a TopSeal. Total assay volume was 16 µL. TR-FRET signal at 665 nm was measured on a M1000 plate reader. Data were calculated and plotted using GraphPad Prism 6 and represent the mean ± SEM of at least three separate determinations.

$G\alpha_{i1}$, $G\alpha_{oA}$ engagement and β-arrestins recruitment

Cell culture and transfections

HEK 293 cells were allowed to grow in high glucose DMEM supplemented with 10% FBS, 100 U/mL penicillin/streptomycin, 2 mM glutamine, and 20mM HEPES at 37˚C in a humidified chamber at 5% CO_2. All transfections were carried out with polyethyleneimine as previously described.[56]

G-Protein engagement and β-arrestin recruitment

HEK293 cells were seeded in T175 flasks. After 24h, cells were transfected with the previously described plasmids coding for hAPJ, $G\alpha_{i1}$-RlucII(91)[48] or $G\alpha_{oA}$-RlucII(99),[57] GFP10-$G\gamma_1$,[48] and $G\beta_1$ (from cDNA.org) or for hAPJ-GFP10[44] and RlucII-β-arrestin-1 or -2.[58]

BRET Experiments

24h after transfection, cells were seeded into white 96 well plates (BD Falcon) at a concentration of 50000 cells/well and incubated at 37˚C overnight. Cells were washed with PBS and 90µL of HBSS was added in each well. Cells were then stimulated with the analog at concentrations ranging from 10^{-6} M to 10^{-12} M for 5 min at 37˚C (G-Proteins) or for 30 min at room temperature (β-arrestins). After stimulation time, 5 µM of coelanterazine 400A was added to each well and the plate was read using the $BRET^2$ filter set of a GeniosPro plate reader (Tecan, Austria). The $BRET^2$ ratio was determined as $GFP10_{em}/RlucII_{em}$. Data were plotted and EC_{50} values were determined by using GraphPad Prism 6. Each data point represent the mean ± SEM of at least three different experiments each done in triplicate.

Blood pressure measurement

Animals

Adult male Sprague Dawley rats (Charles River Laboratories, St-Constant, Quebec, Canada) were maintained on a 12 h light/12 h dark cycle with access to food and water *ad libitum*. The experimental procedures in this study were approved by the Animal Care Committee of the Université de Sherbrooke and were in accordance with policies and directives of the Canadian Council on Animal Care.

Hypotensive effects

Sprague-Dawley male rats (300-400g) were anaesthetized with a mixture of ketamine and xylazine (87:13 mg/kg intramuscular) and placed on a heating pad. Then, the systolic, diastolic, and mean arterial pressures were measured every 30 seconds by the tail-cuff method, using the CODA Blood Pressure System (Kent Scientific Co., Connecticut, USA). When the blood pressure has stabilized (five consecutive measure with less than 5% variability), apelin-13 or Tyr(OBn) analog **12** (0.001, 0.01, 0.1, or 1 mg/kg, in 300 µL of saline) was injected via the tail vein. Blood pressure measurements were acquired for seven minutes following the injection.

ACKNOWLEDGMENTS

Financial support from Université de Sherbrooke, the Natural Sciences and Engineering Research Council of Canada (Collaborative Research & Development Grant with Tranzyme Pharma), TranzymePharma, and the FRQS-funded Réseau Québécois de Recherche sur le Médicament (RQRM) is acknowledged. The Institut de Pharmacologie de Sherbrooke (IPS) and the FRQNT-funded Proteo network are also acknowledged for scholarship and travel grants to A.M. M.A.-M. is the recipient of a Heart and Stroke Foundation of Canada (HFSC) New Investigator award. P.S. is the recipient of the Canada Research Chair in Neurophysiopharmacology of Chronic Pain.

SUPPORTING INFORMATION AVAILABLE

Analytical high performance liquid chromatography (HPLC) and High Resolution Mass Spectrometry (HRMS) spectra of the different compounds described in this manuscript are presented in the supporting information. This material is available free of charge via the Internet at http://pubs.acs.org.

REFERENCES

(1) O'Dowd, B. F.; Heiber, M.; Chan, A.; Heng, H. H.; Tsui, L. C.; Kennedy, J. L.; Shi, X.; Petronis, A.; George, S. R.; Nguyen, T. A Human Gene That Shows Identity with the Gene Encoding the Angiotensin Receptor Is Located on Chromosome 11. *Gene* **1993**, *136*, 355–360.

(2) De Mota, N.; Reaux-Le Goazigo, A.; El Messari, S.; Chartrel, N.; Roesch, D.; Dujardin, C.; Kordon, C.; Vaudry, H.; Moos, F.; Llorens-Cortes, C. Apelin, a Potent Diuretic Neuropeptide Counteracting Vasopressin Actions through Inhibition of Vasopressin Neuron Activity and Vasopressin Release. *Proc. Natl. Acad. Sci. U. S. A.* **2004**, *101*, 10464–10469.

(3) Zhen, E. Y.; Higgs, R. E.; Gutierrez, J. a. Pyroglutamyl Apelin-13 Identified as the Major Apelin Isoform in Human Plasma. *Anal. Biochem.* **2013**, *442*, 1–9.

(4) O'Carroll, a M.; Selby, T. L.; Palkovits, M.; Lolait, S. J. Distribution of mRNA Encoding B78/apj, the Rat Homologue of the Human APJ Receptor, and Its Endogenous Ligand Apelin in Brain and Peripheral Tissues. *Biochim. Biophys. Acta* **2000**, *1492*, 72–80.

(5) Hosoya, M.; Kawamata, Y.; Fukusumi, S.; Fujii, R.; Habata, Y.; Hinuma, S.; Kitada, C.; Honda, S.; Kurokawa, T.; Onda, H.; et al. Molecular and Functional Characteristics of APJ. Tissue Distribution of mRNA and Interaction with the Endogenous Ligand Apelin. *J. Biol. Chem.* **2000**, *275*, 21061–21067.

(6) Medhurst, A. D.; Jennings, C. a.; Robbins, M. J.; Davis, R. P.; Ellis, C.; Winborn, K. Y.; Lawrie, K. W. M.; Hervieu, G.; Riley, G.; Bolaky, J. E.; et al. Pharmacological and Immunohistochemical Characterization of the APJ Receptor and Its Endogenous Ligand Apelin. *J. Neurochem.* **2003**, *84*, 1162–1172.

(7) Lee, D. K.; Cheng, R.; Nguyen, T.; Fan, T.; Kariyawasam, a P.; Liu, Y.; Osmond, D. H.; George, S. R.; O'Dowd, B. F. Characterization of Apelin, the Ligand for the APJ Receptor. *J. Neurochem.* **2000**, *74*, 34–41.

(8) Reaux, a; De Mota, N.; Skultetyova, I.; Lenkei, Z.; El Messari, S.; Gallatz, K.; Corvol, P.; Palkovits, M.; Llorens-Cortès, C. Physiological Role of a Novel Neuropeptide, Apelin, and Its Receptor in the Rat Brain. *J. Neurochem.* **2001**, *77*, 1085–1096.

(9) Falcão-Pires, I.; Ladeiras-Lopes, R.; Leite-Moreira, A. F. The Apelinergic System: A Promising Therapeutic Target. *Expert Opin. Ther. Targets* **2010**, *14*, 633–645.

(10) O'Carroll, A.-M.; Lolait, S. J.; Harris, L. E.; Pope, G. R. The Apelin Receptor APJ: Journey from an Orphan to a Multifaceted Regulator of Homeostasis. *J. Endocrinol.* **2013**, *219*, R13–R35.

(11) Scimia, M. C.; Hurtado, C.; Ray, S.; Metzler, S.; Wei, K.; Wang, J.; Woods, C. E.; Purcell, N. H.; Catalucci, D.; Akasaka, T.; et al. APJ Acts as a Dual Receptor in Cardiac Hypertrophy. *Nature* **2012**, *488*, 394–398.

(12) Szokodi, I.; Tavi, P.; Földes, G.; Voutilainen-Myllylä, S.; Ilves, M.; Tokola, H.; Pikkarainen, S.; Piuhola, J.; Rysä, J.; Tóth, M.; et al. Apelin, the Novel Endogenous Ligand of the Orphan Receptor APJ, Regulates Cardiac Contractility. *Circ. Res.* **2002**, *91*, 434–440.

(13) Berry, M. F.; Pirolli, T. J.; Jayasankar, V.; Burdick, J.; Morine, K. J.; Gardner, T. J.; Woo, Y. J. Apelin Has in Vivo Inotropic Effects on Normal and Failing Hearts. *Circulation* **2004**, *110*, II187–II193.

(14) Chamberland, C.; Barajas-Martinez, H.; Haufe, V.; Fecteau, M.-H.; Delabre, J.-F.; Burashnikov, A.; Antzelevitch, C.; Lesur, O.; Chraibi, A.; Sarret, P.; et al. Modulation of Canine Cardiac Sodium Current by Apelin. *J. Mol. Cell. Cardiol.* **2010**, *48*, 694–701.

(15) Japp, A. G.; Cruden, N. L.; Amer, D. a B.; Li, V. K. Y.; Goudie, E. B.; Johnston, N. R.; Sharma, S.; Neilson, I.; Webb, D. J.; Megson, I. L.; et al. Vascular Effects of Apelin in Vivo in Man. *J. Am. Coll. Cardiol.* **2008**, *52*, 908–913.

(16) Japp, a G.; Cruden, N. L.; Barnes, G.; van Gemeren, N.; Mathews, J.; Adamson, J.; Johnston, N. R.; Denvir, M. a; Megson, I. L.; Flapan, a D.; et al. Acute Cardiovascular Effects of Apelin in Humans: Potential Role in Patients with Chronic Heart Failure. *Circulation* **2010**, *121*, 1818–1827.

(17) Barnes, G. D.; Alam, S.; Carter, G.; Pedersen, C. M.; Lee, K. M.; Hubbard, T. J.; Veitch, S.; Jeong, H.; White, A.; Cruden, N. L.; et al. Sustained Cardiovascular Actions of APJ Agonism during Renin-Angiotensin System Activation and in Patients with Heart Failure. *Circ. Heart Fail.* **2013**, *6*, 482–491.

(18) Tatemoto, K.; Hosoya, M.; Habata, Y.; Fujii, R.; Kakegawa, T.; Zou, M. X.; Kawamata, Y.; Fukusumi, S.; Hinuma, S.; Kitada, C.; et al. Isolation and Characterization of a Novel Endogenous Peptide Ligand for the Human APJ Receptor. *Biochem. Biophys. Res. Commun.* **1998**, *251*, 471–476.

(19) El Messari, S.; Iturrioz, X.; Fassot, C.; De Mota, N.; Roesch, D.; Llorens-Cortes, C. Functional Dissociation of Apelin Receptor Signaling and Endocytosis: Implications for the Effects of Apelin on Arterial Blood Pressure. *J. Neurochem.* **2004**, *90*, 1290–1301.

(20) Kuba, K.; Zhang, L.; Imai, Y.; Arab, S.; Chen, M.; Maekawa, Y.; Leschnik, M.; Leibbrandt, A.; Markovic, M.; Makovic, M.; et al. Impaired Heart Contractility in Apelin Gene-Deficient Mice Associated with Aging and Pressure Overload. *Circ. Res.* **2007**, *101*, e32–e42.

(21) Charles, C. J. Update on Apelin Peptides as Putative Targets for Cardiovascular Drug Discovery. *Expert Opin. Drug Discov.* **2011**, *6*, 633–644.

(22) Scimia, M. C.; Blass, B. E.; Koch, W. J. Apelin Receptor: Its Responsiveness to Stretch Mechanisms and Its Potential for Cardiovascular Therapy. *Expert Rev. Cardiovasc. Ther.* **2014**, *12*, 733–741.

(23) Lee, D. K.; Saldivia, V. R.; Nguyen, T.; Cheng, R.; George, S. R.; O'Dowd, B. F. Modification of the Terminal Residue of Apelin-13 Antagonizes Its Hypotensive Action. *Endocrinology* **2005**, *146*, 231–236.

(24) Vickers, C.; Hales, P.; Kaushik, V.; Dick, L.; Gavin, J.; Tang, J.; Godbout, K.; Parsons, T.; Baronas, E.; Hsieh, F.; et al. Hydrolysis of Biological Peptides by Human Angiotensin-Converting Enzyme-Related Carboxypeptidase. *J. Biol. Chem.* **2002**, *277*, 14838–14843.

(25) Habata, Y.; Fujii, R.; Hosoya, M.; Fukusumi, S.; Kawamata, Y.; Hinuma, S.; Kitada, C.; Nishizawa, N.; Murosaki, S.; Kurokawa, T.; et al. Apelin, the Natural Ligand of the Orphan Receptor APJ, Is Abundantly Secreted in the Colostrum. *Biochim. Biophys. Acta* **1999**, *1452*, 25–35.

(26) Yue, P.; Jin, H.; Xu, S.; Aillaud, M.; Deng, A. C.; Azuma, J.; Kundu, R. K.; Reaven, G. M.; Quertermous, T.; Tsao, P. S. Apelin Decreases Lipolysis via G(q), G(i), and AMPK-Dependent Mechanisms. *Endocrinology* **2011**, *152*, 59–68.

(27) Li, Y.; Chen, J.; Bai, B.; Du, H.; Liu, Y.; Liu, H. Heterodimerization of Human Apelin and Kappa Opioid Receptors: Roles in Signal Transduction. *Cell. Signal.* **2012**, *24*, 991–1001.

(28) Bai, B.; Tang, J.; Liu, H.; Chen, J.; Li, Y.; Song, W. Apelin-13 Induces ERK1/2 but Not p38 MAPK Activation through Coupling of the Human Apelin Receptor to the Gi2 Pathway. *Acta Biochim. Biophys. Sin. (Shanghai).* **2008**, *40*, 311–318.

(29) Masri, B.; Morin, N.; Pedebernade, L.; Knibiehler, B.; Audigier, Y. The Apelin Receptor Is Coupled to Gi1 or Gi2 Protein and Is Differentially Desensitized by Apelin Fragments. *J. Biol. Chem.* **2006**, *281*, 18317–18326.

(30) Lee, D. K.; Ferguson, S. S. G.; George, S. R.; O'Dowd, B. F. The Fate of the Internalized Apelin Receptor Is Determined by Different Isoforms of Apelin Mediating Differential Interaction with Beta-Arrestin. *Biochem. Biophys. Res. Commun.* **2010**, *395*, 185–189.

(31) Iturrioz, X.; Gerbier, R.; Leroux, V.; Alvear-Perez, R.; Maigret, B.; Llorens-Cortes, C. By Interacting with the C-Terminal Phe of Apelin, Phe255 and Trp259 in Helix VI of the Apelin Receptor Are Critical for Internalization. *J. Biol. Chem.* **2010**, *285*, 32627–32637.

(32) Ceraudo, E.; Galanth, C.; Carpentier, E.; Banegas-Font, I.; Schonegge, A.-M.; Alvear-Perez, R.; Iturrioz, X.; Bouvier, M.; Llorens-Cortes, C. Biased Signaling Favoring Gi over B-Arrestin Promoted by an Apelin Fragment Lacking the C-Terminal Phenylalanine. *J. Biol. Chem.* **2014**, *289*, 24599–24610.

(33) Langelaan, D. N.; Bebbington, E. M.; Reddy, T.; Rainey, J. K. Structural Insight into G-Protein Coupled Receptor Binding by Apelin. *Biochemistry* **2009**, *48*, 537–548.

(34) Fan, X.; Zhou, N.; Zhang, X.; Mukhtar, M.; Lu, Z.; Fang, J.; DuBois, G. C.; Pomerantz, R. J. Structural and Functional Study of the Apelin-13 Peptide, an

Endogenous Ligand of the HIV-1 Coreceptor, APJ. *Biochemistry* **2003**, *42*, 10163–10168.

(35) Gerbier, R.; Leroux, V.; Couvineau, P.; Alvear-Perez, R.; Maigret, B.; Llorens-Cortes, C.; Iturrioz, X. New Structural Insights into the Apelin Receptor: Identification of Key Residues for Apelin Binding. *FASEB J.* **2015**, *29*, 314–322.

(36) Hamada, J.; Kimura, J.; Ishida, J.; Kohda, T.; Morishita, S.; Ichihara, S.; Fukamizu, A. Evaluation of Novel Cyclic Analogues of Apelin. *Int. J. Mol. Med.* **2008**, *22*, 547–552.

(37) Macaluso, N. J. M.; Glen, R. C. Exploring the "RPRL" Motif of Apelin-13 through Molecular Simulation and Biological Evaluation of Cyclic Peptide Analogues. *ChemMedChem* **2010**, *5*, 1247–1253.

(38) Macaluso, N. J. M.; Pitkin, S. L.; Maguire, J. J.; Davenport, A. P.; Glen, R. C. Discovery of a Competitive Apelin Receptor (APJ) Antagonist. *ChemMedChem* **2011**, *6*, 1017–1023.

(39) Iturrioz, X.; Alvear-Perez, R.; De Mota, N.; Franchet, C.; Guillier, F.; Leroux, V.; Dabire, H.; Le Jouan, M.; Chabane, H.; Gerbier, R.; et al. Identification and Pharmacological Properties of E339-3D6, the First Nonpeptidic Apelin Receptor Agonist. *FASEB J.* **2010**, *24*, 1506–1517.

(40) Margathe, J.-F.; Iturrioz, X.; Alvear-Perez, R.; Marsol, C.; Riché, S.; Chabane, H.; Tounsi, N.; Kuhry, M.; Heissler, D.; Hibert, M.; et al. Structure-Activity Relationship Studies toward the Discovery of Selective Apelin Receptor Agonists. *J. Med. Chem.* **2014**, *57*, 2908–2919.

(41) Murza, A.; Belleville, K.; Longpré, J.-M.; Sarret, P.; Marsault, E. Stability and Degradation Patterns of Chemically Modified Analogs of Apelin-13 in Plasma and Cerebrospinal Fluid. *Biopolymers* **2014**, *102*, 297–303.

(42) Zhang, Y.; Maitra, R.; Harris, D. L.; Dhungana, S.; Snyder, R.; Runyon, S. P. Identifying Structural Determinants of Potency for Analogs of Apelin-13: Integration of C-Terminal Truncation with Structure-Activity. *Bioorg. Med. Chem.* **2014**, *22*, 2992–2997.

(43) Wang, W.; McKinnie, S. M. K.; Patel, V. B.; Haddad, G.; Wang, Z.; Zhabyeyev, P.; Das, S. K.; Basu, R.; McLean, B.; Kandalam, V.; et al. Loss of Apelin Exacerbates Myocardial Infarction Adverse Remodeling and Ischemia-Reperfusion Injury: Therapeutic Potential of Synthetic Apelin Analogues. *J. Am. Heart Assoc.* **2013**, *2*, e000249.

(44) Murza, A.; Parent, A.; Besserer-Offroy, E.; Tremblay, H.; Karadereye, F.; Beaudet, N.; Leduc, R.; Sarret, P.; Marsault, É. Elucidation of the Structure-Activity Relationships of Apelin: Influence of Unnatural Amino Acids on Binding, Signaling, and Plasma Stability. *ChemMedChem* **2012**, *7*, 318–325.

(45) Vogt, W. Oxidation of Methionyl Residues in Proteins: Tools, Targets, and Reversal. *Free Radic. Biol. Med.* **1995**, *18*, 93–105.

(46) Black, J. W.; Leff, P. Operational Models of Pharmacological Agonism. *Proc. R. Soc. Lond. B. Biol. Sci.* **1983**, *220*, 141–162.

(47) Limbird, L. E. *Cell Surface Receptors: A Short Course on Theory and Methods*; Springer.; 2005; p. 23.

(48) Galés, C.; Van Durm, J. J. J.; Schaak, S.; Pontier, S.; Percherancier, Y.; Audet, M.; Paris, H.; Bouvier, M. Probing the Activation-Promoted Structural Rearrangements in Preassembled Receptor-G Protein Complexes. *Nat. Struct. Mol. Biol.* **2006**, *13*, 778–786.

(49) Buck, J.; Sinclair, M. L.; Schapal, L.; Cann, M. J.; Levin, L. R. Cytosolic Adenylyl Cyclase Defines a Unique Signaling Molecule in Mammals. *Proc. Natl. Acad. Sci. U. S. A.* **1999**, *96*, 79–84.

(50) Sunahara, R. K.; Taussig, R. Isoforms of Mammalian Adenylyl Cyclase: Multiplicities of Signaling. *Mol. Interv.* **2002**, *2*, 168–184.

(51) Birnbaumer, L. Expansion of Signal Transduction by G Proteins. The Second 15 Years or so: From 3 to 16 Alpha Subunits plus Betagamma Dimers. *Biochim. Biophys. Acta* **2007**, *1768*, 772–793.

(52) Ehrlich, A. T.; Furuyashiki, T.; Kitaoka, S.; Kakizuka, A.; Narumiya, S. Prostaglandin E Receptor EP1 Forms a Complex with Dopamine D1 Receptor and Directs D1-Induced cAMP Production to Adenylyl Cyclase 7 through Mobilizing G(βγ) Subunits in Human Embryonic Kidney 293T Cells. *Mol. Pharmacol.* **2013**, *84*, 476–486.

(53) Marques, F. D.; Ferreira, A. J.; Sinisterra, R. D. M.; Jacoby, B. A.; Sousa, F. B.; Caliari, M. V; Silva, G. A. B.; Melo, M. B.; Nadu, A. P.; Souza, L. E.; et al. An Oral Formulation of Angiotensin-(1-7) Produces Cardioprotective Effects in Infarcted and Isoproterenol-Treated Rats. *Hypertension* **2011**, *57*, 477–483.

(54) Tatemoto, K.; Takayama, K.; Zou, M. X.; Kumaki, I.; Zhang, W.; Kumano, K.; Fujimiya, M. The Novel Peptide Apelin Lowers Blood Pressure via a Nitric Oxide-Dependent Mechanism. *Regul. Pept.* **2001**, *99*, 87–92.

(55) Cheng, Y.; Prusoff, W. H. Relationship between the Inhibition Constant (K1) and the Concentration of Inhibitor Which Causes 50 per Cent Inhibition (I50) of an Enzymatic Reaction. *Biochem. Pharmacol.* **1973**, *22*, 3099–3108.

(56) Ehrhardt, C.; Schmolke, M.; Matzke, A.; Knoblauch, A.; Will, C.; Wixler, V.; Ludwig, S. Polyethylenimine, a Cost-Effective Transfection Reagent. *Signal Transduct.* **2006**, *6*, 179–184.

(57) Richard-Lalonde, M.; Nagi, K.; Audet, N.; Sleno, R.; Amraei, M.; Hogue, M.; Balboni, G.; Schiller, P. W.; Bouvier, M.; Hébert, T. E.; et al. Conformational Dynamics of Kir3.1/Kir3.2 Channel Activation via Δ-Opioid Receptors. *Mol. Pharmacol.* **2013**, *83*, 416–428.

(58) Zimmerman, B.; Beautrait, A.; Aguila, B.; Charles, R.; Escher, E.; Claing, A.; Bouvier, M.; Laporte, S. A. Differential B-Arrestin-Dependent Conformational Signaling and Cellular Responses Revealed by Angiotensin Analogs. *Sci. Signal.* **2012**, *5*, ra33.

This is the accepted version of the following article: Murza A, et al. (2015), J Med Chem, 58(5):2431-40, **which has been published in final form at** http://pubs.acs.org/doi/abs/10.1021/jm501916k

Table 1. Characterization of Phe[13] modified analogs of apelin-13

N°	Sequence	Mol. formula	Purity % [a]	Theoretical mass	Exact mass measured [b]
Ape13	<Glu-R-P-R-L-S-H-K-G-P-M-P-F	$C_{69}H_{108}N_{22}O_{16}S$	100.0	1532.8034	1532.8116
1	<Glu-R-P-R-L-S-H-K-G-P-**Nle**-P-F	$C_{70}H_{110}N_{22}O_{16}$	100.0	1514.8470	1514.8502
2	<Glu-R-P-R-L-S-H-K-G-P-**Nle**-P-**I**	$C_{67}H_{112}N_{22}O_{16}$	100.0	1480.8627	1480.8723
3	<Glu-R-P-R-L-S-H-K-G-P-**Nle**-P-**L**	$C_{67}H_{112}N_{22}O_{16}$	98.6	1480.8627	1480.8702
4	<Glu-R-P-R-L-S-H-K-G-P-**Nle**-P-**V**	$C_{66}H_{110}N_{22}O_{16}$	100.0	1466.8470	1466.8857
5	<Glu-R-P-R-L-S-H-K-G-P-**Nle**-P-**Tyr(OMe)**	$C_{71}H_{112}N_{22}O_{17}$	100.0	1544.8576	1544.8635
6	<Glu-R-P-R-L-S-H-K-G-P-**Nle**-P-**Phe(4-Me)**	$C_{71}H_{112}N_{22}O_{16}$	100.0	1528.8627	1528.8696
7	<Glu-R-P-R-L-S-H-K-G-P-**Nle**-P-**(4-pyridyl)Ala**	$C_{69}H_{109}N_{23}O_{16}$	100.0	1515.8423	1515.8502
8	<Glu-R-P-R-L-S-H-K-G-P-**Nle**-P-**(3-pyridyl)Ala**	$C_{69}H_{109}N_{23}O_{16}$	100.0	1515.8423	1515.8505
9	<Glu-R-P-R-L-S-H-K-G-P-**Nle**-P-**(2-pyridyl)Ala**	$C_{69}H_{109}N_{23}O_{16}$	100.0	1515.8423	1515.8523
10	<Glu-R-P-R-L-S-H-K-G-P-**Nle**-P-**Phg**	$C_{69}H_{108}N_{22}O_{16}$	100.0	1500.8314	1500.8391
11	<Glu-R-P-R-L-S-H-K-G-P-**Nle**-P-**hPhe**	$C_{71}H_{112}N_{22}O_{16}$	100.0	1528.8627	1528.8732
12	<Glu-R-P-R-L-S-H-K-G-P-**Nle**-P-**Tyr(OBn)**	$C_{77}H_{116}N_{22}O_{17}$	97.1	1620.8889	1620.8967
13	<Glu-R-P-R-L-S-H-K-G-P-**Nle**-P-**Bpa**	$C_{77}H_{114}N_{22}O_{17}$	100.0	1618.8732	1618.8834
14	<Glu-R-P-R-L-S-H-K-G-P-**Nle**-P-**StyrylAla**	$C_{72}H_{112}N_{22}O_{16}$	100.0	1540.8627	1540.8690
15	<Glu-R-P-R-L-S-H-K-G-P-**Nle**-P-**dihydroAnthranylAla**	$C_{78}H_{116}N_{22}O_{16}$	99.6	1616.8940	1616.8950
16	<Glu-R-P-R-L-S-H-K-G-P-**Nle**-P-**(3-benzothienyl)Ala**	$C_{72}H_{110}N_{22}O_{16}S$	100.0	1570.8191	1570.8294
17	<Glu-R-P-R-L-S-H-K-G-P-**Nle**-P-**(α-Me)Phe**	$C_{71}H_{112}N_{22}O_{16}$	98.9	1528.8627	1528.8729
18	<Glu-R-P-R-L-S-H-K-G-P-**Nle**-P-**(D-α-Me)Phe**	$C_{71}H_{112}N_{22}O_{16}$	97.4	1528.8627	1528.8723
19	<Glu-R-P-R-L-S-H-K-G-P-**Nle**-P-**Aminoindane**	$C_{71}H_{110}N_{22}O_{16}$	100.0	1526.8470	1526.8563
20	R-L-S-H-K-G-P-**Nle**-P-**Tyr(OBn)**	$C_{61}H_{92}N_{16}O_{13}$	100.0	1256.7030	1256.7117
21	S-H-K-G-P-**Nle**-P-**Tyr(OBn)**	$C_{49}H_{69}N_{11}O_{11}$	97.7	987.5178	987.5214
22	K-G-P-**Nle**-P-**Tyr(OBn)**	$C_{40}H_{57}N_7O_8$	99.4	763.4269	763.4318
23	P-**Nle**-P-**Tyr(OBn)**	$C_{32}H_{42}N_4O_6$	98.0	578.3104	578.3126

[a] Purity determined by HPLC-UV at 223 nm. [b] Exact mass determined by High Resolution Mass Spectrometry (HRMS).

This is the accepted version of the following article: Murza A, et al. (2015), J Med Chem, 58(5):2431-40, **which has been published in final form at** http://pubs.acs.org/doi/abs/10.1021/jm501916k

Table 2. Phe[13] modified analogs of apelin-13 and results on binding affinity and functional assays

N°	Sequence	Binding		Functional Assays	
		IC_{50} (nM)[a]	K_i (nM)[b]	cAMP EC_{50} (nM)[c]	$G\alpha_i$ EC_{50} (nM)[d]
Ape13	Pyr-R-P-R-L-S-H-K-G-P-M-P-F	1.2 ± 0.1	1.0 ± 0.1	1.4 ± 0.1	0.84 ± 0.25
1	Pyr-R-P-R-L-S-H-K-G-P-**Nle**-P-F	2.6 ± 0.6	2.1 ± 0.5	4.5 ± 1.5	0.53 ± 0.14
2	Pyr-R-P-R-L-S-H-K-G-P-**Nle**-P-**I**	11.4 ± 1.0	9.1 ± 0.8	3.1 ± 0.5	2.5 ± 1.1
3	Pyr-R-P-R-L-S-H-K-G-P-**Nle**-P-**L**	7.9 ± 0.8	6.3 ± 0.6	2.9 ± 0.5	1.3 ± 0.5
4	Pyr-R-P-R-L-S-H-K-G-P-**Nle**-P-**V**	18.2 ± 3.2	14.6 ± 2.6	4.7 ± 1.3	2.7 ± 1.5
5	Pyr-R-P-R-L-S-H-K-G-P-**Nle**-P-**Tyr(OMe)**	0.60 ± 0.05	0.48 ± 0.04	0.23 ± 0.05	1.3 ± 0.6
6	Pyr-R-P-R-L-S-H-K-G-P-**Nle**-P-**Phe(4-Me)**	0.25 ± 0.02	0.20 ± 0.02	0.17 ± 0.1	1.4 ± 0.9
7	Pyr-R-P-R-L-S-H-K-G-P-**Nle**-P-**(4-pyridyl)Ala**	1.3 ± 0.2	1.0 ± 0.2	0.45 ± 0.1	0.73 ± 0.46
8	Pyr-R-P-R-L-S-H-K-G-P-**Nle**-P-**(3-pyridyl)Ala**	1.6 ± 0.1	1.3 ± 0.1	2.3 ± 1.0	2.0 ± 1.3
9	Pyr-R-P-R-L-S-H-K-G-P-**Nle**-P-**(2-pyridyl)Ala**	6.1 ± 1.0	4.9 ± 0.8	3.6 ± 1.4	3.0 ± 1.4
10	Pyr-R-P-R-L-S-H-K-G-P-**Nle**-P-**Phg**	14.3 ± 1.4	11.4 ± 1.1	2.7 ± 0.4	4.2 ± 2.0
11	Pyr-R-P-R-L-S-H-K-G-P-**Nle**-P-**hPhe**	6.7 ± 1.1	5.4 ± 0.9	0.24 ± 0.06	1.4 ± 0.5
12	Pyr-R-P-R-L-S-H-K-G-P-**Nle**-P-**Tyr(OBn)**	0.02 ± 0.003	0.016 ± 0.002	0.35 ± 0.09	1.1 ± 0.5
13	Pyr-R-P-R-L-S-H-K-G-P-**Nle**-P-**Bpa**	0.48 ± 0.05	0.38 ± 0.04	0.04 ± 0.02	0.91 ± 0.32
14	Pyr-R-P-R-L-S-H-K-G-P-**Nle**-P-**StyrylAla**	1.5 ± 0.2	1.2± 0.2	0.63 ± 0.2	3.4 ± 2.4
15	Pyr-R-P-R-L-S-H-K-G-P-**Nle**-P-**dihydroAnthranylAla**	13.7 ± 1.6	11.0 ± 1.3	95 ± 19	6.0 ± 2.4
16	Pyr-R-P-R-L-S-H-K-G-P-**Nle**-P-**(3-benzothienyl)Ala**	2.8 ± 0.4	2.2 ± 0.3	1.3 ± 0.4	1.3 ± 1.2
17	Pyr-R-P-R-L-S-H-K-G-P-**Nle**-P-**(α-Me)Phe**	0.43 ± 0.03	0.34 ± 0.02	0.07 ± 0.02	2.7 ± 1.1
18	Pyr-R-P-R-L-S-H-K-G-P-**Nle**-P-**(D-α-Me)Phe**	0.86 ± 0.16	0.69 ± 0.13	0.86 ± 0.17	2.8 ± 0.5
19	Pyr-R-P-R-L-S-H-K-G-P-**Nle**-P-**Aminoindane**	1.7 ± 0.1	1.4 ± 0.1	1.1 ± 0.2	1.4 ± 0.8

[a] Concentration producing 50% competitive inhibition of binding of radioligand apelin-13[Glp^{65}, Nle^{75}, Tyr^{77}][^{125}I], values represent the mean ± S.E.M. of three determinations. [b] Inhibition constants (K_i) of analogs calculated using the Cheng-Prusoff equation. [c] Concentration that produces 50% inhibition of forskolin-induced cAMP accumulation, values represent the mean ± S.E.M. of three determinations. [d] Concentration that produces 50% dissociation of $G\alpha_{i1}$ subunit as observed in BRET assay, values represent the mean ± S.E.M. of three determinations.

Table 3. Truncated derivatives of the Tyr(OBn) analog

N°	Sequence	Binding IC_{50} (nM)[a]	Binding K_i (nM)[b]
12	Pyr-R-P-R-L-S-H-K-G-P-**Nle**-P-**Tyr(OBn)**	0.02 ± 0.003	0.016 ± 0.002
20	R-L-S-H-K-G-P-**Nle**-P-**Tyr(OBn)**	57 ± 11	46 ± 9
21	S-H-K-G-P-**Nle**-P-**Tyr(OBn)**	> 10 000	> 10 000
22	K-G-P-**Nle**-P-**Tyr(OBn)**	> 10 000	> 10 000
23	P-**Nle**-P-**Tyr(OBn)**	> 10 000	> 10 000

[a] Concentration producing 50% competitive inhibition of binding of radioligand apelin-13[Glp^{65}, Nle^{75}, Tyr^{77}][^{125}I],values represent the mean ± S.E.M. of two determinations. [b] Inhibitions constants (K_i) of analogs calculated using Cheng-Prusoff equation.

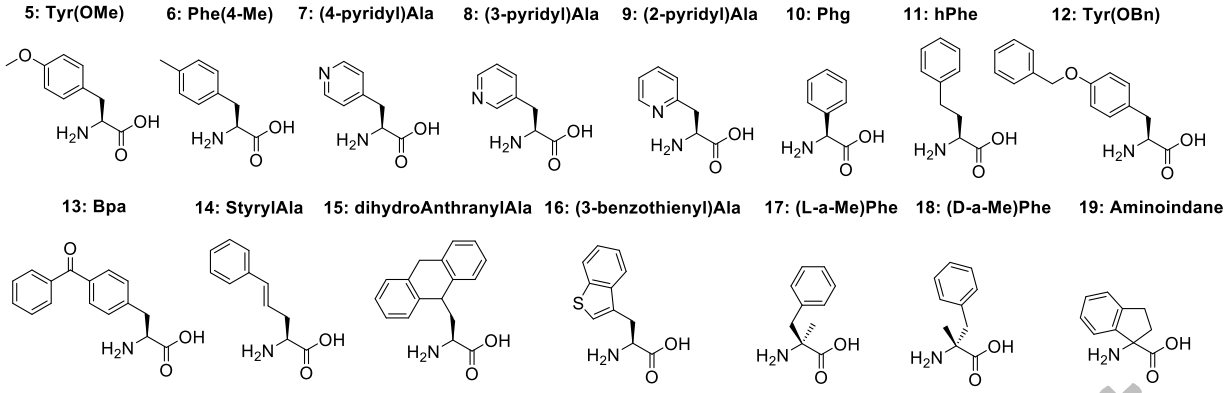

Figure 1. Chemical structures of unnatural amino acids used in this study.

A

EC_{50} (nM)	Apelin-13	12
cAMP	1.4 ± 0.1	0.35 ± 0.09 **
$G\alpha_{i1}$	0.84 ± 0.25	1.1 ± 0.5
$G\alpha_{oA}$	5.9 ± 0.6	1.4 ± 0.5 **
β-arrestin-1	26 ± 3.1	7.4 ± 0.8 **
β-arrestin-2	29 ± 9.8	13 ± 1.9

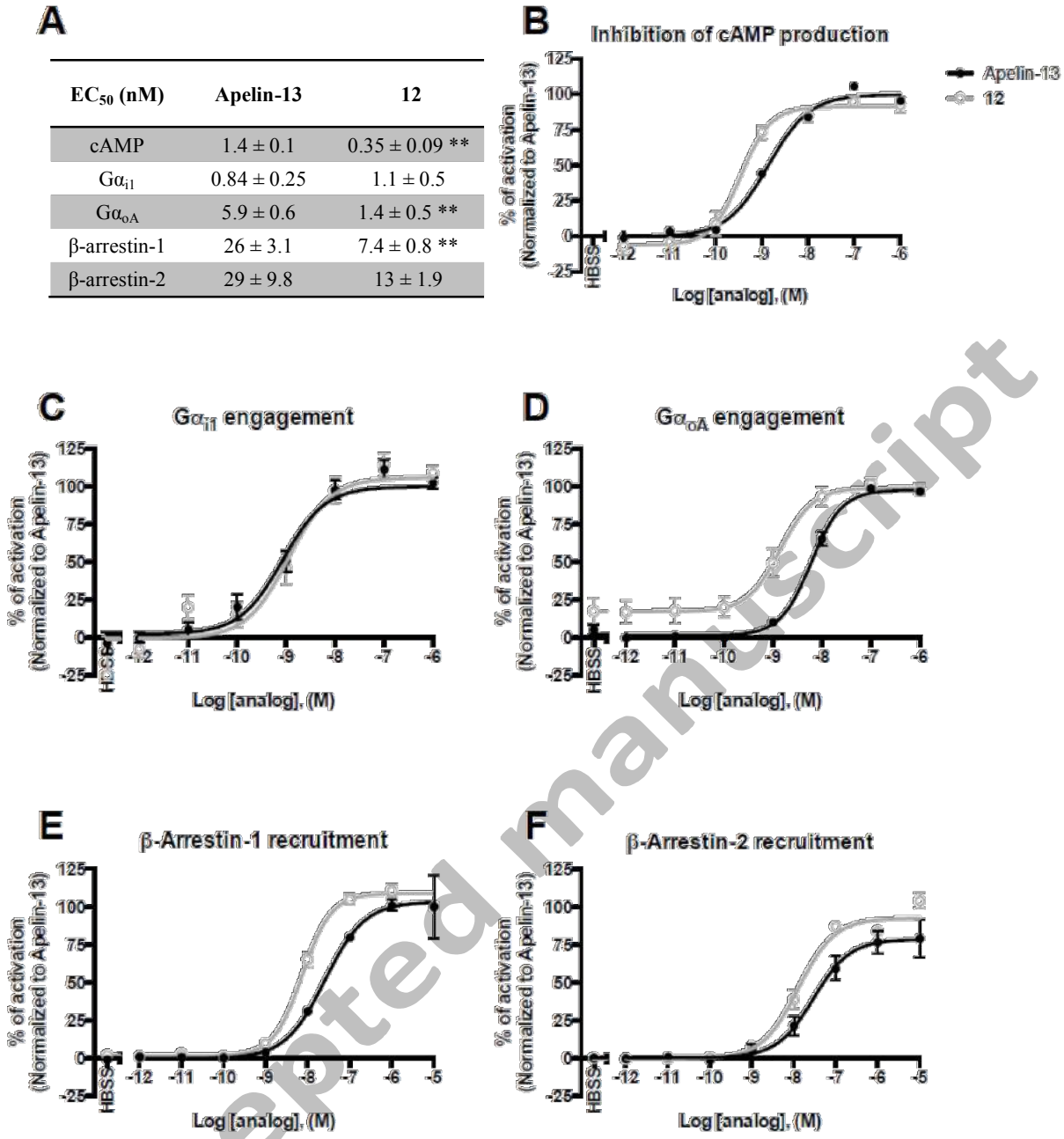

Figure 2. Potency (EC_{50}) and concentration-response curves of apelin-13 and Tyr(OBn) analog **12** on cAMP production, $G\alpha_{i/o}$ engagement and β-arrestins recruitment. (A) EC_{50} of apelin-13 and compound **12** are represented. Concentration-response relationships of apelin-13 and (**12**) for thei rability: (B) to inhibit the forskolin-induced cAMP production; (C) to engage $G\alpha_{i1}$ and; (D) to engage $G\alpha_{oA}$. Apelin-13 and (**12**) were also assessed for their ability to trigger the recruitment of: (E) β-arrestin-1 and; (F) β-arrestin-2. Statistical analyses were performed with a two tailed Student t-test. ** $p < 0.01$ vs. apelin-13.

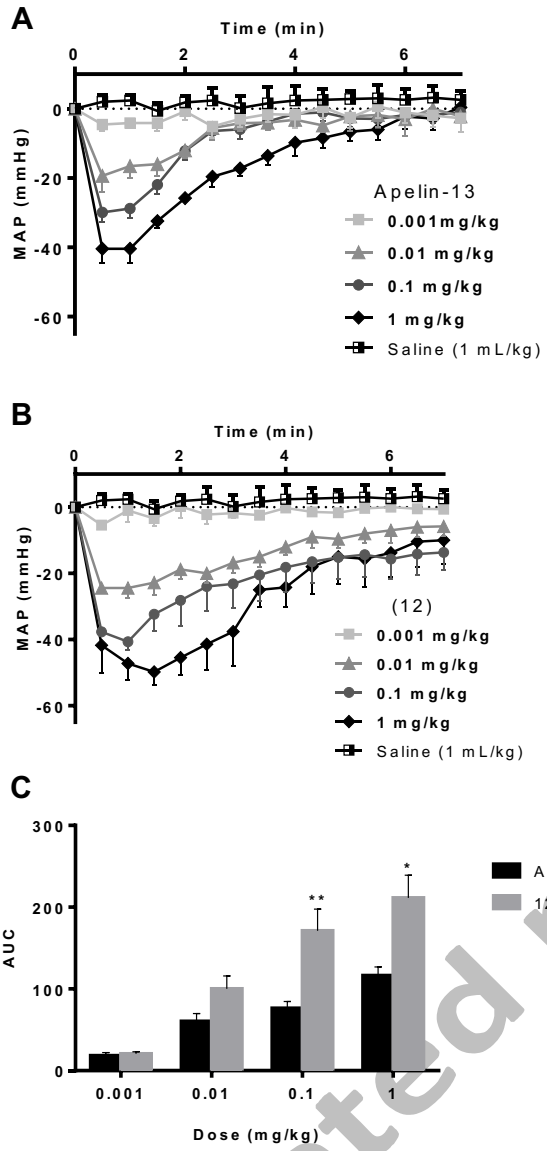

Figure 3. Effects of apelin-13 and Tyr(OBn)[13] analog **12** on blood pressure in anesthetized rats. Tracings depicting the hypotensive effects of (A) apelin-13 and (B) **12** in rats, when given as a bolus via the tail vein. (C) Histograms showing the area under the curve (AUC) of the mean arterial pressure (MAP) decrease induced by administration of increasing doses (0.001, 0.01, 0.1, and 1 mg/kg) of apelin-13 and **12**. Each bar represents the average value ± S.E.M. obtained with 6–8 animals. Statistical analyses were performed with a Mann-Whitney test. *p <0.05, ** p <0.01 vs. apelin-13.

TABLE OF CONTENT GRAPHIC

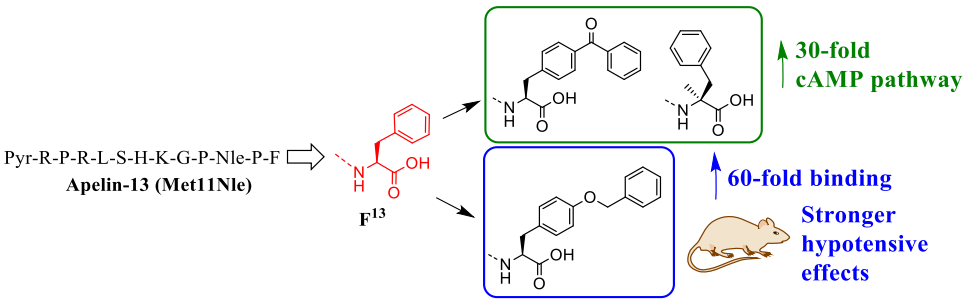

For Table of Contents only